Estimation of site charge distribution in organic conductors, α- and θ-(BEDT-TTF)$_2$I$_3$, under hydrostatic pressure (BEDT-TTF: bis(ethylenedithio)tetrathiafulvalene)

Kyuya YAKUSHI,[a,b]* R. WOJCIECHOWSKI,[b] Kaoru YAMAMOTO,[b]
Toshihiro HIEJIMA,[c] and Atsushi KAWAMOTO[d]

[a]*Toyota Physical and Chemical Research Institute, 41-1, Yokomichi, Nagakute, Aichi, 480-1192, Japan*
[b]*Institute for Molecular Science, 38 Nishigonaka, Myodaiji, Okazaki, Aichi 444-8585 Japan*
[c]*Department of Nanochemistry, Faculty of Engineering, Tokyo Polytechnic University, 1583 Iiyama, Atsugi 243-0297, Japan*
[d]*Department of Physics, Hokkaido University, Kita-Ku, Sapporo, 060-0810 Japan*

Abstract

We present the assignment of the C=C stretching modes, ν_2 and ν_3 of α- and θ-(BEDT-TTF)$_2$I$_3$ and α-(BEDT-TTF)$_2$NH$_4$Hg(SCN)$_4$ with the aid of ^{13}C- and deuterium-substituted compounds. To estimate the site charge at around 0.5, we present an empirical relation between the frequency of ν_2 mode and site charge. The relationship was examined by applying it to α- and θ-(BEDT-TTF)$_2$I$_3$ and α-(BEDT-TTF)$_2$NH$_4$Hg(SCN)$_4$ in a metallic phase at ambient pressure. Based on the assignment and empirical relation, we estimated the site-charge distribution of α- and θ-(BEDT-TTF)$_2$I$_3$ under hydrostatic pressure. On increasing pressure, the site-charge distribution of α-(BEDT-TTF)$_2$I$_3$ tends to approach uniform distribution, while θ-(BEDT-TTF)$_2$I$_3$ keeps the uniform site-charge distribution up to 3.1GPa.

Introduction

More than 200 charge-transfer salts have been synthesized combining BEDT-TTF and various counter anions. Among the various known organic conductors,[1,2] α-(BEDT-TTF)$_2$I$_3$ (BEDT-TTF = bis(ethylenedithio) tetrathiafulvalene, abbreviated as ET hereafter) shows various electronic properties such as charge ordering[3], super-conductivity[4], a zero-gap state (ZGS)[5,6], photo-induced phase transition[7], and non-linear optical response[8]. α-(ET)$_2$I$_3$ exhibits a first-order metal-insulator (MI) phase transition at T_{MI} = 135 K.[9] Based on theoretical[10,11,12], ^{13}C-NMR[13,14], Raman[15], infrared[16], and x-ray[17] studies, the insulating phase is regarded as a charge-ordered (CO) state. The crystal structure of α-(ET)$_2$I$_3$ consists of alternating anion and donor layers.[9] The donor layer has a herringbone arrangement of ET molecules. The unit cell accommodates two holes (plus charges), they are allocated to four ET molecules named A, A', B, and C. The hole number allocated to each site corresponds to the valence of molecule or fractional site charge. In the metallic phase, A and A' are connected by inversion symmetry, and B and C are located on the inversion center. In the CO phase, on the other hand, the holes are redistributed so as to reduce the intersite Coulomb energy, and they are split into two charge-rich and two charge-poor sites, which breaks inversion symmetry.[8] It has been reported in α-(ET)$_2$I$_3$ that the site-charge distribution is non-uniform even in the metallic phase,[15,16,17] although the average hole number per a site is 0.5 in the case of uniform distribution.

The non-uniform site charge has been interpreted from the tight-binding[15] and extended Hubbard models[18]. The fractional charge at *j*th site, ρ_j, is calculated by the equation $\rho_j = \sum_{ka,kb}^{4}\sum_{m}\langle km|n_j|km\rangle f(\varepsilon)$ where $|km\rangle$ is the Bloch function of the *m*th band, n_j is the number operator at the *j*th site, and $f(\varepsilon)$ is the Fermi distribution function for a hole. The equation (1) implies that the site charge reflects the overall band structure, which is described by a transfer integral *t* and Coulomb energy *U* and *V*. Therefore, the site charge verifies the quality of the band calculation. However, the site charge, especially under high pressure, has not been reliably examined experimentally. Raman spectroscopy is a powerful method to estimate the site charge, ρ_j, if we carefully analyze the charge-sensitive mode (ν_2 mode in ET). In addition the Raman experiment under high pressure is easier than infrared experiment.

The MI transition of α-(ET)$_2$I$_3$ is suppressed by hydrostatic pressure. It has been recognized that the transport properties such as Hall coefficient and magnetoresistance above 1.5GPa are interpreted by ZGS with a Dirac cone dispersion.[5,6] The crystal structure of θ-(ET)$_2$I$_3$ also consists of a herringbone arrangement of ET molecules. The unit cell consists of two

2012年1月31日 受理
*豊田理化学研究所フェロー

conducting layer of ET separated by I_3^- layer. The arrangement of ET in a single conducting layer resembles that of α-(ET)$_2$I$_3$, while the four ET molecules are practically equivalent to each other.[19] Application of hydrostatic pressure induces metal-to-ZGS phase transition.[20,21] Raman spectroscopic study of θ-(ET)$_2$I$_3$ as well as α-(ET)$_2$I$_3$ will give some insight into the electronic state under high pressure. To interpret the high-pressure Raman spectrum of α-(ET)$_2$I$_3$, we conduct reliable assignment for the C=C stretching vibration of α-(ET)$_2$I$_3$ with the aid of ^{13}C- and deuterium-substituted compounds. Isostructural α-(ET)$_2$NH$_4$Hg(SCN)$_4$ is also examined, for the reason that the Raman bands of α-(ET)$_2$I$_3$ is very broadened and unresolved due to the fluctuation of charge order.[16] Based on the assignment, we estimate the site hole number of α-(ET)$_2$I$_3$, α-(ET)$_2$NH$_4$Hg-(SCN)$_4$, and θ-(ET)$_2$I$_3$ in a metallic phase. Finally, we present the pressure dependent site hole numbers of α-(ET)$_2$I$_3$ and θ-(ET)$_2$I$_3$.

Experimental techniques

Single crystals of α-(ET)$_2$I$_3$ were grown by a standard electrochemical method in a tetrahydrofuran solution of ET (^{13}C-substituted ET, and deuterium-substituted ET) and tetrabuthylammonium triiodide ((*t*-Bu)$_4$N-I$_3$). In ^{13}C- substituted ET, the carbon atoms at the central C=C bridge were substituted by ^{13}C. In deuterium-substituted ET, all hydrogen atoms in ethylene end groups were substituted by deuterium. In the following discussion, the charge-transfer salt of ^{13}C (deuterium)-substituted ET is denoted as α-(^{13}C-ET)$_2$X$_3$ (α-(d$_8$-ET)$_2$X$_3$). In the process of electrochemical crystallization, the single crystals of θ-(ET)$_2$I$_3$ was harvested on a rare occasion. The single crystal of α-(ET)$_2$-NH$_4$Hg(SCN)$_4$ was obtained following the electrochemical crystallization method described in ref. [22]. The crystal face and axes were determined by x-ray diffraction using a Rigaku Mercury CCD diffractometer.

Raman spectra were obtained using a Renishaw Ramascope System-1000 in backscattering geometry. Lasers for excitation were focused on an area *ca.* 50 μm in diameter at powers in the range 100–80 μW. An analyzer was not used for the scattered light. Details of the low-temperature experiment including the high-pressure technique were described elsewhere.[23] A polarized reflection spectrum was obtained using a Nicolet Nexus 870 FT-IR spectrometer combined with a microscope (Spectratech IR-Plan). For the low-temperature experiment, a small goniometer head was attached to the cold head of the cryostat (Oxford CF1104s), which was fixed to an XYZ stage. The details of the experimental methods have been described previously.[24]

Results and Discussion

Assignment of the C=C stretching modes of α-(ET)$_2$I$_3$ in a chargeorder

Figure 1 shows infrared and Raman spectra of α-(ET)$_2$I$_3$, α-(d$_8$-ET)$_2$I$_3$, and α-(^{13}C-ET)$_2$I$_3$, all in the CO state. In this spectral region, ET has three C=C stretching modes: ν_2: the in-phase ring C=C stretching is mixed with bridge C=C stretching in an out-of-phase fashion, ν_3: the bridge C=C stretching is mixed with in-phase ring C=C stretching in an in-phase fashion, and ν_{27}: the out-of-phase ring C=C stretching. The ν_{27} mode is perturbed by site charges, the ν_2 mode is perturbed mainly by site charges, and the ν_3 mode is mainly perturbed by intersite transfer interactions.[25] Through interaction with the electronic state, these vibrational and vibronic modes are split into four, as the unit cell contains four BEDT-TTF molecules. The notations $\nu_{j\mathrm{P}}^i$ and $\nu_{j\mathrm{R}}^i$ (j=2, 27; i=1, 2) were respectively defined as the i-th ν_j mode at charge-poor and charge-rich sites, and ν_3^i (i=1–4) was defined as the i-th ν_3 mode.

We followed the assignments of ref. [15], except for the Raman bands at 1476 cm^{-1} and 1462 cm^{-1}, which had been assigned to ν_3^1 and $\nu_{2\mathrm{R}}^2$, respectively. Since the isotope shift of ν_2 and ν_3 became closer to each other within each mode,

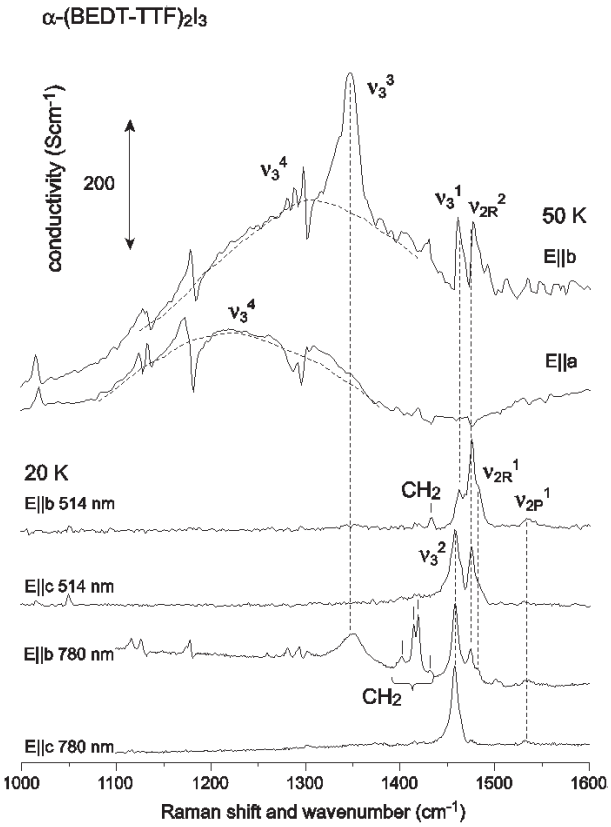

Fig. 1a Optical conductivity polarized along the *b* and *a* directions and Raman spectra of α-(ET)$_2$I$_3$.

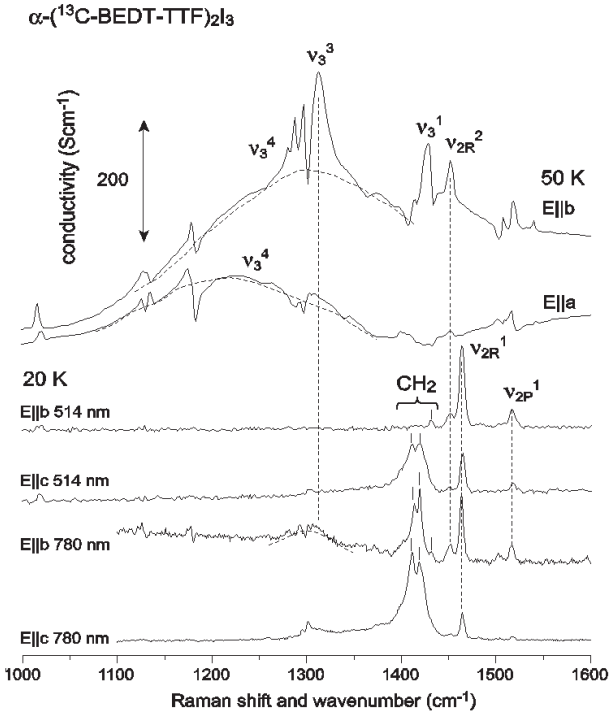

Fig. 1b Optical conductivity polarized along the *b* and *a* directions and Raman spectra of α-(^{13}C-ET)$_2$I$_3$.

we interchanged the assignment as shown in Table 1. Since ν^1_{2R} and ν^2_{2R} are close to ν^1_3, they are mixed with each other. Therefore, the ν^1_{2R} and ν^2_{2R} cannot be used for estimating site hole number of charge rich sites. The vibronic modes in the conducting plane were assigned with the aid of isotope shift and comparison with the Raman spectrum. The vibronic modes ν^2_{2R}, ν^1_3, and ν^3_3 in the optical conductivity spectra were unambiguously assigned as shown in Figs. 1a and 1b. The very broad band, in which the peak was different between the E$\|a$ and E$\|b$ spectra, was assigned to ν^4_3, since the frequency of the vibronic mode depended upon the electronic excitation spectrum. If the unit cell has inversion symmetry, the Raman-active band cannot be observed in infrared spectrum and *vice versa*. As shown in Table 1, ν^2_{2R}, $\nu_3{}^1$, and ν^3_3 are found in both the Raman and infrared spectra, which violate the mutual exclusion rule. This observation provides clear evidence for the breaking of center of symmetry.

Assignment of the C=C stretching modes of metallic α- and θ-(ET)$_2$I$_3$ and α-(ET)$_2$NH$_4$Hg(SCN)$_4$

Figure 2 shows the Raman spectra of metallic α-(ET)$_2$I$_3$, metallic α-(ET)$_2$NH$_4$Hg(SCN)$_4$, and θ-(ET)$_2$I$_3$. The former two compounds are isostructural to each other. α-(ET)$_2$I$_3$ is semi-metallic above 135 K, while α-(ET)$_2$NH$_4$Hg(SCN)$_4$ is metallic down to a low temperature, and shows superconductivity at 1 K.[26] As well as α-(ET)$_2$I$_3$, the unit cell of α-(ET)$_2$NH$_4$Hg(SCN)$_4$ with space group $P\bar{1}$ involves four ET molecules (see Fig. 1 of ref. [22] for the definition of A, A', B, and C). For the same reason described in the previous subsection, three modes of ν_2 and ν_3 are Raman active, and one of ν_2 and ν_3 is infrared active. In the case of α-(ET)$_2$I$_3$, two ν_2 modes were observed, whereas three ν_2 were observed in ^{13}C-substitued compound as shown in Figs. 2a, 2a', 2b, and 2b'. From the isotope shift, we can safely assign three bands to ν^1_2, ν^3_2, and ν^1_3 modes, and, ν^2_2 is missing from Fig. 2a. In the case of α-(ET)$_2$NH$_4$Hg(SCN)$_4$, three ν_2 and two ν_3 modes were observed and they were unambiguously assigned through the isotope shift shown in Figs. 2c and 2c'. However, another Raman-active ν_3 mode was missing from the Raman spectrum.

θ-(ET)$_2$I$_3$ is metallic down to low temperature and undergoes superconducting transition at 3.6 K.[27] The crystal belong to monoclinic system with space group of $P2_1/c$, and

Table 1. Assignment of the infrared and Raman modes of α-(BEDT-TTF)$_2$I$_3$.[a]

	Raman (20K)		infrared (50K)	
	α-(^{12}C-ET)$_2$I$_3$	α-(^{13}C-ET)$_2$I$_3$	α-(^{12}C-ET)$_2$I$_3$	α-(^{13}C-ET)$_2$I$_3$
ν^1_{2P}	1536	1517 [19]		(1518?)
ν^2_{2P}				(1508?)
ν^1_{2R}	1483	1465 [18]		
ν^2_{2R}	1476	1452 [24]	1477	1454 [23]
ν^1_3	1462		1462	1431 [31]
ν^2_3	1458			
ν^3_3	1349	1315 [34]	1346	1315 [31]
ν^4_3			~1300 (E$\|b$)	~1300 (E$\|b$)
			~1230 (E$\|a$)	~1230 (E$\|a$)
CH_2–Bending	1431	1431		
	1419	1420		
	1414	1414		
	1402	1402		

[a] The numerical value in parenthesis shows the isotope shift, $\Delta\nu_j = \nu_j^{12} - \nu_j^{13}$.

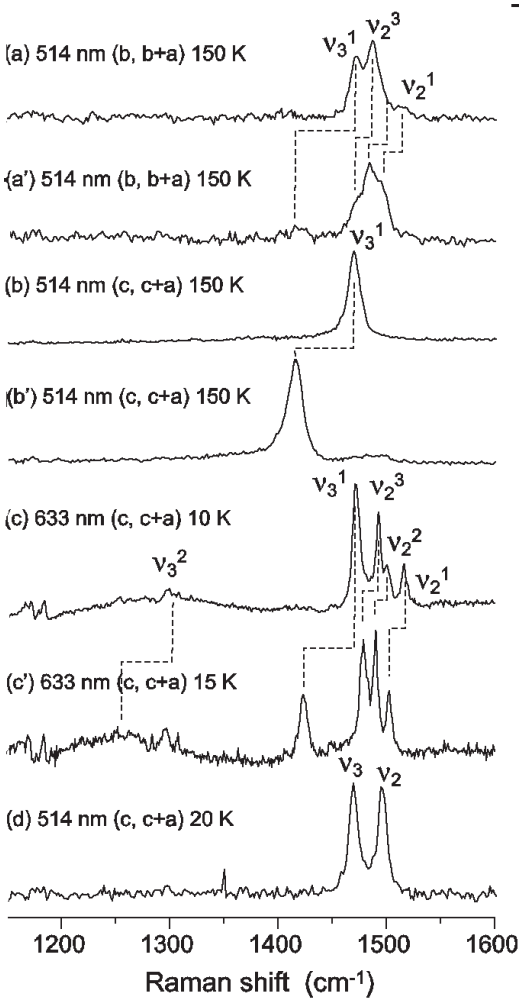

Fig. 2 Raman spectra of α-(ET)$_2$I$_3$ and α-(ET)$_2$NH$_4$Hg(SCN)$_4$, and the ^{13}C-substitued compound, in which two carbon atoms of the central C=C bond of BEDT-TTF were substituted by ^{13}C. (a) and (b) α-(ET)$_2$I$_3$, (a') and (b') α-(^{13}C-ET)$_2$I$_3$, (c) α-(ET)$_2$NH$_4$Hg(SCN)$_4$, (c') α-(^{13}C-ET)$_2$NH$_4$Hg (SCN)$_4$, and (d) θ-(ET)$_2$I$_3$.

the unit cell contains 4 ET molecules. However, the arrangement of ET molecules is actually described by orthorhombic system with space group *P*nma with the unit cell of crystallographically equivalent two ET molecules.[28] Due to the high symmetry of the unit cell, the Raman spectrum shown in Fig. 2d is very simple. Two peaks are unambiguously assigned to ν_2 and ν_3 as shown in Fig. 3d. The frequencies of ν_2 and ν_3 modes of these compounds were shown in Table 2.

Relation between frequency and site hole number

The relationship between frequency of the ν_2 mode of ET and the valence of ET, which corresponds to the site hole number, ρ, was examined in ref. [25]. They assumed a linear relationship in the range of $0 \le \rho \le 0.8$.[29] The ρ dependence of the frequency of ν_2 mode is ascribed to ρ dependent force constant $F(\rho)$. That is, the linear relationship requires $(dF/d\rho)_{\rho=0} = (dF/d\rho)_{\rho=1}$.[30] However, the frequency of $ET^{0.5+}$ is significantly deviated from the linear relationship toward low-frequency side, which means that $|(dF/d\rho)_{\rho=0}| > |(dF/d\rho)_{\rho=1}|$. To estimate the site charge more reliably at around $\rho = 0.5$, we propose the following empirical equation, $\nu_2(\rho) = 1570 - 180\rho + 57\rho^2$ ($\rho \sim 0.5$), where $\nu_2(0) = 1570$ cm^{-1} for the calculated frequency of flat neutral ET molecule, $\nu_2(0.5) = 1494$ cm^{-1}, 1494 cm^{-1}, 1495 cm^{-1} respectively for β'-(ET)$_2$ICl$_2$, κ-(ET)$_2$Cu$_2$CN$_3$, and κ-(ET)$_2$Cu[N(CN)$_2$]Cl at room temperature, and $\nu_2(1) = 1447$ cm^{-1} for (ET)ClO$_4$ and (ET)AuBr$_2$Cl$_2$ at room temperature.[31] All of the compound with $\rho = 0.5$ shows blue shift by about 6 cm^{-1} from room temperature to 10 K, due to the hardening of crystal lattice. The temperature dependence is described by the following empirical equation $\nu_2(0.5, T) = A/\cosh(T/B)$ ($0 < T < 300$ K). The example for the ν_2 mode of κ-(ET)$_2$Cu[N(CN)$_2$]$_2$ is displayed in Fig. 3.

If we assume $\nu_2(0)$ and $\nu_2(1)$ also show the same temperature dependence, the quadratic expression can be corrected as

$$\nu_2(\rho) = 1576/\cosh(T/3500) - 180\rho + 57\rho^2 \qquad (1)$$

for $T < 300$ K. However, the temperature dependence of molecular vibration is not simple but depends upon the compound. For example, the ν_2 mode of θ-(ET)$_2$I$_3$ shifts less than 3 cm^{-1} at 10 K. We therefore estimate the ambiguity of the site hole number as $6/123 \approx 0.05$.

Table 2. Assignment of the Raman modes of α-(ET)$_2$I$_3$, α-(ET)$_2$NH$_4$Hg(SCN)$_4$, and θ-(ET)$_2$I$_3$

	α-(^{12}C-ET)$_2$NH$_4$Hg(SCN)$_4$	α-(^{13}C-ET)$_2$NH$_4$Hg(SCN)$_4$	isotope shift	α-(^{12}C-ET)$_2$I$_3$	α-(^{13}C-ET)$_2$I$_3$	isotope shift	θ-(ET)$_2$I$_3$
	Raman (10K)	Raman (15K)	$\Delta\nu = \nu^{12} - \nu^{13}$	Raman (150K)	Raman (150K)	$\Delta\nu = \nu_3^{12} - \nu^{13}$	Raman (20K)
ν_2^1	1515	1503	13	1516	1496	~20	
ν_2^2	1500	1490	10	—	~1484	—	1496
ν_2^3	1492	1479	14	1487	1470	17	
ν_3^1	1471	1423	48	1471	~1415	56	
ν_3^2	—	—	—	—	—	—	1469
ν_3^3	~1300	~1250	~50	—	—	—	
ν_3^4	—	—	—	—	—	—	

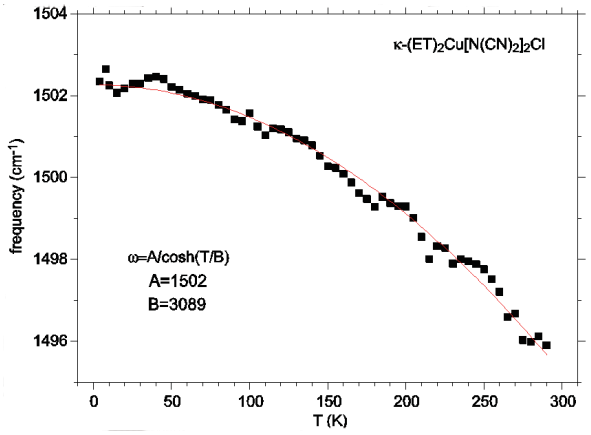

Fig. 3 Temperature dependence of the frequency of ν_2 of κ-$(ET)_2Cu[N(CN)_2]_2Cl$. The solid line is the best fit equation, $\omega = A/\cosh(T/B)$.

Site charges of metallic α- and θ-$(ET)_2I_3$, α-$(ET)_2NH_4Hg(SCN)_4$, at ambient pressure

Using the equation (1), we estimated the site charge (hole number) of the metallic state of α-$(ET)_2I_3$ from the frequency of ν_2 listed in Table 2. The site charges at 150 K are 0.60 and 0.37. According to the x-ray diffraction study, the site charge follows the order, $\rho_B > \rho_A = \rho_{A'} > \rho_C$, in the metallic state.[17] If we assume that 0.60 and 0.37 corresponds to the hole numbers of the sites B and C, respectively, the hole number of site A = A' is estimated to be 0.52. This assumption is consistent with the above order for the site hole number, and the assignment that ν_2^2 is missing in α-$(ET)_2I_3$ (*See* Fig. 2(a) and 2(a')). The non-uniform site charge is significantly smaller than the CO amplitude of α-$(ET)_2I_3$ in the CO state[16]. The origin of the site-charge distribution in CO state is different from that in metallic state. In the former state, the site-charge distribution is ruled by intersite Coulomb interaction, whereas in the latter it is mainly by non-equivalent transfer integrals around the site. The anion potential may contribute to make non-uniform site charges. On this point, Katayama *et al*. showed that anion potential gives a small influence on the site charge.[32] Kobayashi *et al*. calculated the temperature dependence of the site hole number within the mean-field approximation for extended Hubbard model.[18] Ishibashi *et al*. made Muliken charge analyses in their *ab initio* calculation of the band structure of α-$(ET)_2I_3$.[33] In Table 3, their results are compared with our experimental result along with the estimation from the molecular geometry determined by x-ray diffraction experiment.[17] The mean-field calculation overestimates the site-charge difference between the site B and site C. In the case of mean-filed approximation, the Coulomb energy parameter, *U*, *Vc*, and *Vp*, enhances the difference in the hole number.[18] Therefore, the Coulomb interaction seems to be more screened in a metallic phase.

Using the equation (1), the site charge of metallic α-$(ET)_2NH_4Hg(SCN)_4$ at 10 K are estimated to be 0.57, 0.50, and 0.39, which are very similar to those of α-$(ET)_2I_3$. As the site charges of α-$(ET)_2NH_4Hg(SCN)_4$ has not been discussed, we calculated the site hole numbers using the mean-field approximation taking the transfer integrals shown in the figure caption of Fig. 4 and Coulomb interaction parameters[18], $U = 0.4$, $Vc = 0.17$, $Vp = 0.05$ eV. The site charge distribution at 10 K was calculated as $\rho_{A(A')} = 0.51$, $\rho_B = 0.47$, $\rho_C = 0.50$, which underestimates the non-uniformity among site charges. As we use the Coulomb interaction parameters same as those for the mean-field calculation of α-$(ET)_2I_3$, this difference is attributed to the transfer integrals. As shown

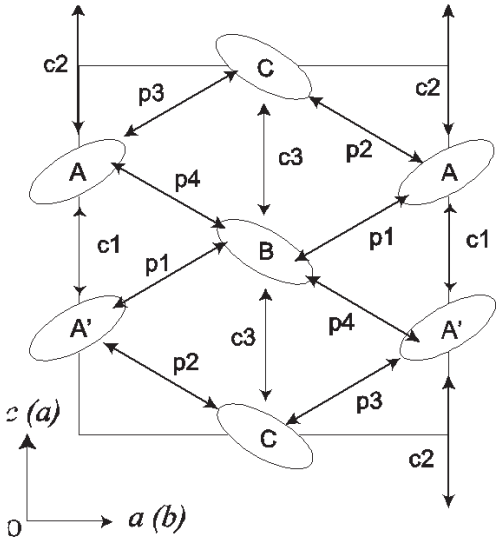

Fig. 4 Transfer integrals of α-$(ET)_2NH_4Hg(SCN)_4$[22] and α-$(ET)_2I_3$[18]). The crystal axes in parentheses correspond to those of α-$(ET)_2I_3$. The parameters are p1 = 0.100 (–0.062), p2 = 0.097 (–0.025), p3 = –0.133 (0.123), p4 = –0.132 (0.140), c1 = 0.019 (–0.020), c2 = –0.068 (0.048), and c3 = 0.013 (–0.028) eV. The numerical values in parentheses correspond to the transfer integrals of α-$(ET)_2I_3$.

Table 3. Site hole density of metallic α-$(ET)_2I_3$

	Raman[a]	x-ray[17]	mean-field theory[18]	ab initio[33]	
	(150K)	(150K)	(150K)	(298K)	(8K)
$n_A = n_{A'}$	(0.52±0.03)	0. 59±0.03	0.52	0.53	0.54
n_B	0.60±0.03	0.67±0.02	0.71	0.55	0.57
n_C	0.37±0.03	0.42±0.02	0.25	0.40	0.37

[a] This work, the error comes from the ambiguity of the empirical equation for estimating site charge.

in Fig. 3, the B (C) site is surrounded by six sites, two A, two A' and two C (B), with transfer integrals, p1 (p2), p4(p3), and c3. The A(A') site is surrounded by two A'(A), two B, and two C sites with transfer integrals, p1, p2, p3, p4, c1, and c2. As shown in the figure caption of Fig. 3, the nearly uniform site charge distribution calculated above comes from the very close set of six transfer integrals around each site. In addition, when the set of transfer integrals is close to each other, Coulomb interaction parameter does enhance the inhomogeneity within the mean-field approximation.[32] Therefore, the nearly uniform site charges calculated by mean-field approximation is attributed to the transfer integral, p1 ≈ p2 ≈ p3 ≈ p4 in α-(ET)$_2$NH$_4$Hg(SCN)$_4$. The estimation of the transfer integrals, especially p1 and p2, should be further examined so as to reproduce more inhomeogeneous sit-charge distribution.

From the symmetry of the unit cell of θ-(ET)$_2$I$_3$, every site is approximately equivalent. Therefore, the site hole number should be 0.5. Applying the empirical equation, the hole number is calculated to be 0.51 at 298 K (1493 cm^{-1}) and 0.54 (1496 cm^{-1}) at 20K. The deviation from 0.5 at 20K comes from the temperature dependence of the ν_2 mode different from κ-type ET salts which are used to obtain the first term of equation (1).

Site hole numbers of θ- and α-(ET)$_2$I$_3$ under hydrostatic pressure

θ-(ET)$_2$I$_3$ undergoes a first order phase transition at around 0.5GPa. The electrical resistance under 1GPa behaves similarly to that of α-(ET)$_2$I$_3$ at the same pressure. In addition, the Hall coefficient shows the same temperature dependence as that of α-(ET)$_2$I$_3$ at the same pressure. These two electrical properties suggest a zero-gap state (ZGS) in θ-(ET)$_2$I$_3$ as well as in α-(ET)$_2$I$_3$. The behavior of the spin shift and spin-lattice relaxation rate in ^{13}C NMR study is also consistent with ZGS.[34] Figure 5 shows the pressure dependence of the Raman spectrum of ν_2 and ν_3 measured at 50K. The Raman spectrum shows a significant blue shift under hydrostatic pressure. However, no distinct change was observed. This result suggests that high symmetry of the unit cell of θ-(ET)$_2$I$_3$ is preserved at least approximately up to 3.1GPa. If this compound is in ZGS above 0.5GPa, there should be a contact point at the Fermi level in band structure which is quite different from that of α-(ET)$_2$I$_3$. The conservation of the pseudo-symmetry provides a restriction when we speculate the crystal and band structure under hydrostatic pressure. The ^{13}C NMR study suggests a structural transformation to α-type structure at 0.5GPa.[34] We speculate that the structural change is very small even if the unit cell symmetry is lowered.

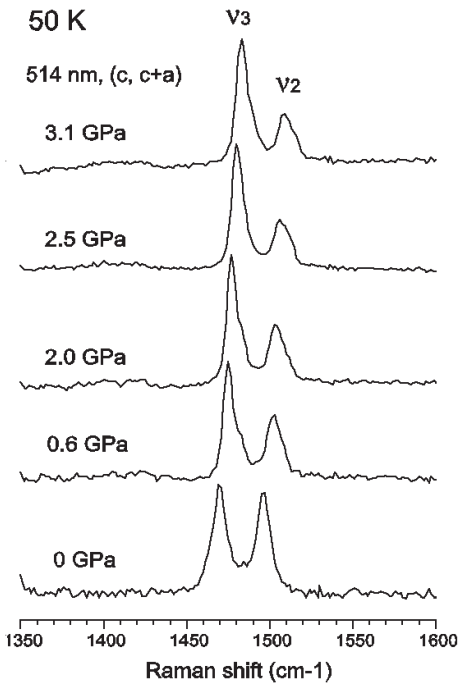

Fig. 5 Pressure dependence of the Raman spectrum of θ-(ET)$_2$I$_3$ measured at 50K.

When the hydrostatic pressure is applied, the molecular vibration shows a blue shift ($\omega + \Delta\omega$). As well as the lattice mode, the frequency shift against pressure is described by $\Delta\omega/\Delta P = \omega\gamma\kappa$, where γ and κ are Gruneisen constant and compressibility, respectively. Therefore, pressure dependent frequency is given by the following equation,

$$\omega(P) = \omega(1 + \gamma\kappa P) \qquad (2).$$

We analyzed the pressure dependence of ν_2 at 20, 50, 100, 150, 200, 250, 300K under the pressure between 0 to 3.2GPa. Since the hydrostatic pressure induces no structural change, we estimated the parameter $\gamma\kappa$. We found that $\gamma\kappa \approx 3 \times 10^{-3}$ GPa^{-1} is approximately temperature independent within the error of 10% in this temperature range as shown in Fig. 6.

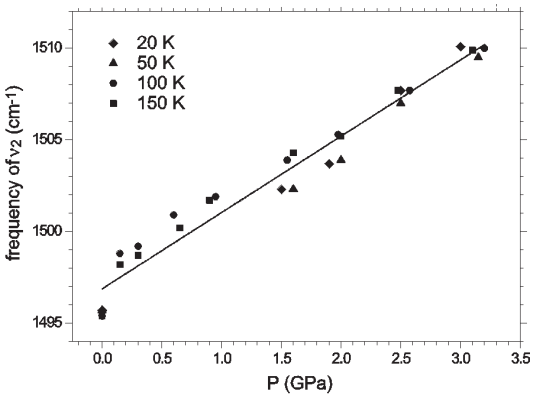

Fig. 6 Pressure dependence of the ν_2 mode of θ-(ET)$_2$I$_3$ at 20K, 50K, 100K, and 150K.

Figure 7 shows the pressure dependence of the Raman spectrum of α-(ET)$_2$I$_3$ at 150K, 100K, and 20K. At 150K, the compound is metallic at ambient pressure. On increasing pressure, the Raman spectrum does not show drastic change. At 100K and 20K, the compound is in a CO phase at ambient pressure. In this case, remarkable spectral changes were found between 0.1GPa and 0.45GPa at 100K and between 1.2GP and 1.5GPa at 20K. These spectral changes correspond to the phase transition from CO phase to metallic phase. In the metallic phase, ν_2^1 and ν_2^2 modes do not show parallel shift, but they tend to merge on increasing pressure. This trend is much more remarkable in the CO phase as shown in Fig. 6c. Hydrostatic pressure not only hardens the lattice but also non-uniformly modulate the transfer integrals, which change the site-charge distribution. Assuming $\gamma\kappa \approx 3\times10^{-3}$GPa^{-1} for α-(ET)$_2I_3$, we estimated the lattice hardening effect on the frequency with the use of equation (2). After eliminating the lattice hardening effect, we estimated the site charge using equation (1). The results are shown in the bottom panel of each figure. In a CO phase, the amplitude of charge order decreases on increasing pressure.[35] This trend is probably associated with the increase of transfer integrals under hydrostatic pressure. In a metallic phase, the site charges approach uniform charge distribution like θ-(ET)$_2$I$_3$ due to a non-uniform increase of transfer integrals on increasing hydrostatic pressure. This result suggests that the crystal structure of zero-gap state of α-(ET)$_2$I$_3$ is slightly modulated so as to equalize the site B and C.

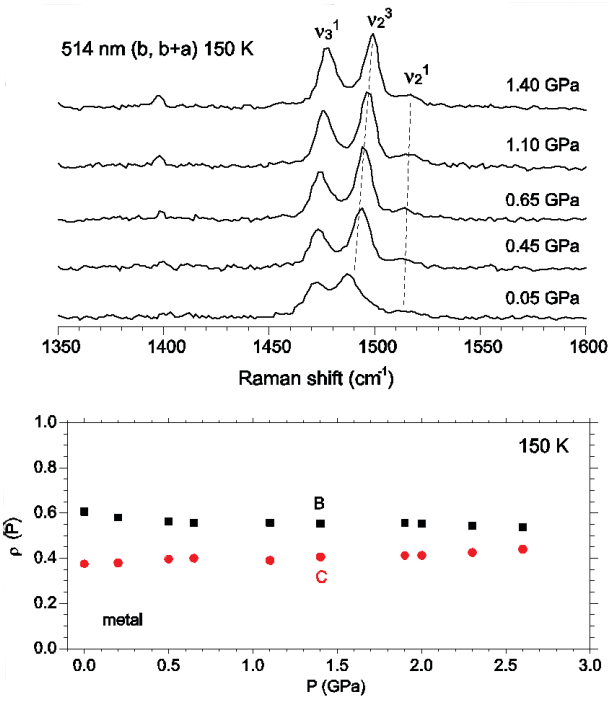

Fig. 7a Pressure dependence of the Raman spectra and hole numbers of θ-(ET)$_2$I$_3$ analyzed at 150K

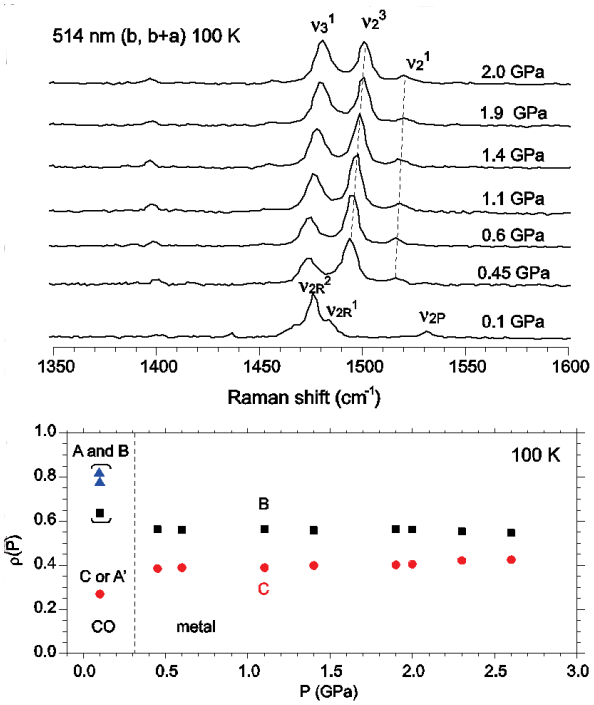

Fig. 7b Pressure dependence of the Raman spectra and hole numbers of θ-(ET)$_2$I$_3$ analyzed at 100K. Ambiguity of the hole numbers at charge-rich site is very large, because ν_{2R} is mixed with ν_3 in the CO state. The symbols, ▲ and ■, in parentheses show the formal hole numbers calculated by equation (1).

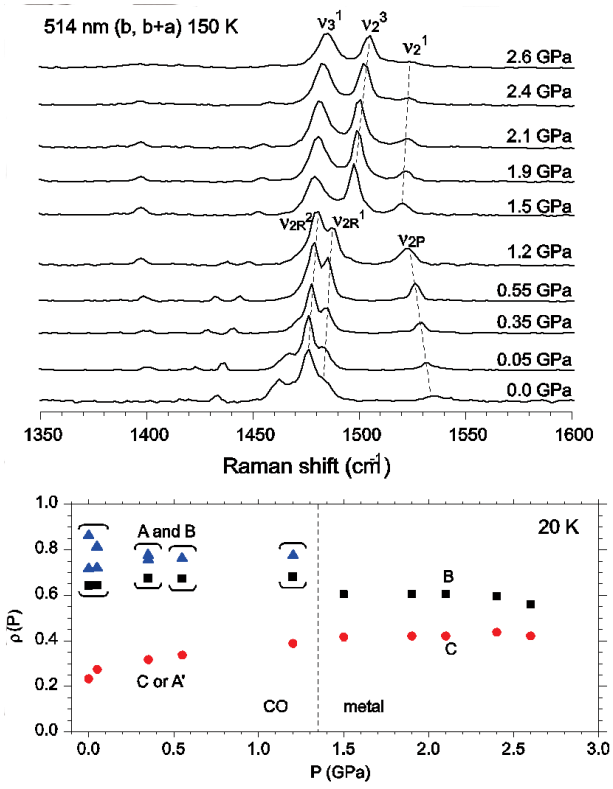

Fig. 7c Pressure dependence of the Raman spectra and hole numbers of α-(ET)$_2$I$_3$ analyzed at 20K. Ambiguity of the hole numbers at charge-rich site is very large, because ν_{2R} is mixed with ν_3 in the CO state. The symbols, ▲ and ■, in parentheses show the formal hole numbers calculated by equation (1).

Conclusion

The Raman bands in the frequency range of C=C stretching modes were assigned with the aid of ^{13}C- and deuterium substituted compounds. The empirical non-linear relationship between ν_2 and site charge was presented taking the temperature dependence into account. Combining the reliable assignment and empirical relation, we estimated the site charges of α-(ET)$_2$I$_3$, α-(ET)$_2$NH$_4$Hg(SCN)$_4$, and θ-(ET)$_2$I$_3$. The non-uniform site-charge distribution of former two compounds in a metallic state resembles each other, whereas the last compound has a uniform site-charge distribution. Hydrostatic pressure seems to show no drastic structural change in θ-(ET)$_2$I$_3$ keeping uniform site-charge distribution, whereas the site-charge distribution of α-(ET)$_2$I$_3$ in a CO state is remarkably changed by hydrostatic pressure. The site charge distribution of metallic α-(ET)$_2$I$_3$ tends to approach a uniform site charge on increasing pressure.

Acknowledgment

We thank Dr. M. Uruichi of Institute for Molecular Science for assisting us in determining the crystal axes by x-ray diffraction technique. This work was partly supported by a Grant-in-Aid for Scientific Research (No.19350074) from MEXT, Japan.

References

[1] *Molecular Conductors: Thematic issue*, *Chem. Rev.* **104**, 4887 (2004).
[2] J. Wosnitza, "*Fermi surfaces of low-dimensional organic metals and superconductors*", Springer (1996).
[3] Y. Takano, K. Hiraki, H.M. Yamamoto, T. Nakamura, and T. Takahashi, *Synth. Met.* **120**, 1081 (2001).
[4] N. Tajima, A. Ebina-Tajima, M. Tamura, Y. Nishio, and K. Kajita, *J. Phys. Soc. Jpn.* **71**, 1832 (2002).
[5] N. Tajima and K. Kajita, *Sci. Technol. Adv. Mater.* 2009, **10**, 024308.
[6] A. Kobayashi, S. Katayama, and Y. Suzumura, *Sci. Technol. Adv. Mater.* 2009, **10**, 024309.
[7] S. Iwai, K. Yamamoto, K. Kashiwazaki, F. Hiramatsu, H. Nakaya, Y. Kawakami, K. Yakushi, H. Okamoto, H. Mori, and Y. Nishio, *Phys. Rev. Lett.* **98**, 097402 (2007).
[8] K. Yamamoto, S. Iwai, S. Boyko, A. Kashiwazaki, F. Hiramatsu, C. Okabe, N. Nishi, and K. Yakushi, *J. Phys. Soc. Jpn.* **77**, 074709 (2008).
[9] K. Bender, I. Henning, D. Schweitzer, K. Dietz, H. Endres and H.J. Keller, *Mol. Cryst. Liq. Cryst.* **108**, 359 (1984).
[10] H. Kino and H. Fukuyama, *J. Phys. Soc. Jpn.* **64**, 1877 (1995).
[11] H. Kino and H. Fukuyama, *J. Phys. Soc. Jpn.* **65**, 2158 (1996).
[12] H. Seo, *J. Phys. Soc. Jpn.* **69**, 805 (2000).
[13] Y. Takano, K. Hiraki, H.M. Yamamoto, T. Nakamura, and T. Takahashi, *Synth. Met.* **120**, 1081 (2001).
[14] T. Takahashi, K. Hiraki, S. Moroto, N. Tajima, Y. Takano, Y. Kubo, H. Satsukawa, R. Chiba, H.M. Yamamoto, R. Kato, and T. Naito, *J. Phys. IV France* **114**, 339 (2004).
[15] R. Wojciechowski, K. Yamamoto, K. Yakushi, M. Inokuchi, and A. Kawamoto, *Phys. Rev.* **B 67**, 224105 (2003).
[16] Y. Yue, K. Yamamoto, M. Uruichi, C. Nakano, K. Yakushi, S. Yamada, T. Hiejima, and A. Kawamoto, *Phys. Rev. B* **82**, 075134 (2010).
[17] T. Kakiuchi, Y. Wakabayashi, H. Sawa, T. Takahashi, and T. Nakamura, *J. Phys. Soc. Jpn.* **76**, 113702 (2007).
[18] A. Kobayashi, S. Katayama, Y. Suzumura, and H. Fukuyama, *J. Phys. Soc. Jpn.* **76**, 034711 (2007).
[19] A. Kobayashi, R. Kato, H. Kobayashi, S. Moriyama, Y. Nishio, K. Kajita, and W. Sasaki, *Chem. Lett.* 2017 (1986).
[20] M. Tamura, F. Matsuzaki, N. Tajima, Y. Nishio, and K. Kajita, *Synth. Met.* **86**, 2007 (1997).
[21] N. Tajima, A. Tajima, M. Tamura, R. Kato, Y. Nishio, and K. Kajita, *J. Phys. IV France* **114**, 263 (2004).
[22] H. Mori, S. Tanaka, M. Oshima, G. Saito, T. Mori, Y. Maruyama, and H. Inoluchi, *Bull. Chem. Soc. Jpn.* **63**, 2183 (1990).
[23] M. Tanaka, K. Yamamoto, M. Uruichi, T. Yamamoto, K. Yakushi, S. Kimura, and H. Mori, *J. Phys. Soc. Jpn.* **77**, 024714 (2008).
[24] K. Yakushi, *Bull. Chem. Soc. Jpn.* **73**, 2643 (2000).
[25] T. Yamamoto, M. Uruichi, K. Yamamoto, K. Yakushi, A. Kawamoto, and H. Taniguchi, *J. Phys. Chem.* **109**, 15226 (2005).
[26] H. Mori, S. Tanaka, K. Oshima, G. Saito, T. Mori, Y. Maruyama, and H. Inokuchi, *Synth. Met.* **41-43**, 2013 (1991).
[27] K. Kajita, Y. Nishio, S. Moriyama, W. Sasaki, R. Kato, H. Kobayashi, and A. Kobayashi, *Solid State Commun.* **64**, 1279 (1987).
[28] A. Kobayashi, R. Kato, H. Kobayashi, S. Moriyama, Y. Nishio, K. Kajita, and W. Sasaki, *Chem. Lett.* 2017 (1986).
[29] See ref. [25] about the reason why this equation is applicable in the range of $0 \leq \rho \leq 0.8$.
[30] Although frequency is proportional to the square root of force constant, the frequency practically linearly depends upon the force constant in a narrow frequency range, $\Delta\omega = \omega(0) - \omega(1)$.
[31] The κ- and β'-ET salts with $\rho = 0.5$ have a dimer unit with large transfer integral. However, the blue shift of ν_2 is not attributed to the emv (electron-molecular-vibration) coupling, because similar blue shift is found in non-dimeric θ-(ET)$_2$I$_3$ which will be shown in the next subsection.
[32] S. Kayatama, A. Kobayashi, and Y. Suzumura, *J. Phys. Conf. Series* **132**, 012003 (2008).
[33] S. Ishibashi, T. Tamura, M. Kohyama, and K. Terakura, *J. Phys. Soc. Jpn.* **75**, 015005 (2006).
[34] K. Miyagawa, M. Hirayama, M. Tamura, and K. Kanoda, *J. Phys. Soc. Jpn.* **79**, 063703 (2010).
[35] The hole numbers shown in the CO state shown in Figs. 5b and 5c are inaccurate, because ν_{2R} is mixed with ν_3^1.